

Dieses Dokument ist eine Zweitveröffentlichung (Postprint) /

This is a self-archiving document (postprint):

Sven Grätz, Doreen Beyer, Valeriya Tkachova, Sarah Hellmann, Reinhard Berger,
Xinliang Feng, Lars Borchardt

The mechanochemical Scholl reaction – a solvent-free and versatile graphitization tool

Erstveröffentlichung in / First published in:

Chemical Communications. 2018, 54 (42), S. 5307 - 5310. Royal Society of Chemistry. ISSN
1364-548X.

DOI: <https://doi.org/10.1039/C8CC01993B>

Diese Version ist verfügbar / This version is available on:

<https://nbn-resolving.org/urn:nbn:de:bsz:14-qucosa2-706550>

The mechanochemical Scholl reaction – a solvent-free and versatile graphitization tool

Sven Grätz^a, Doreen Beyer^b, Valeriya Tkachova^b, Sarah Hellmann^a, Reinhard Berger^b, Xinliang Feng^b and Lars Borchardt^{*a}

^a Professur für Anorganische Chemie I, TU Dresden,
Bergstraße 66, D-01069 Dresden, Germany.

^b Professur für molekulare Funktionsmaterialien, TU Dresden, Mommsenstr. 4, D-01069 Dresden, Germany.

† Footnotes relating to the title and/or authors should appear here.

Electronic Supplementary Information (ESI) available: [details of any supplementary information available should be included here]. See DOI: 10.1039/x0xx00000x

Herein, we report on the mechanochemical Scholl reaction of dendritic oligophenylene precursors to produce benchmark nanographenes such as hexa-peri-hexabenzocoronene (HBC), triangular shaped C₆₀ and expanded C₂₂₂ under solvent-free conditions. The solvent-free approach overcomes the bottleneck of solubility limitation in this well-known and powerful reaction. The mechanochemical approach allows tracking the reaction process by in situ pressure measurements. The quality of produced nanographenes has been confirmed by MALDI-TOF mass spectrometry and UV-Vis absorption spectroscopy. This approach paves the way towards gram scale and environmentally benign synthesis of extended nanographenes and possibly graphene nanoribbons suitable for application in carbon based electronics or energy applications.

The Scholl reaction^{1–3}, a Lewis-acid catalysed oxidative cyclodehydrogenation forming aryl-aryl bonds, is at the heart of bottom-up synthesis of polycyclic aromatic hydrocarbons (PAHs)⁴ or nanographenes and graphene nanoribbons (GNRs).⁵ These materials have been studied extensively in the last century predominantly because of their semiconducting properties and potential applications in organic electronics. In contrast to thermally activated cyclodehydrogenation in on-surface synthesis,^{6–8} the solution-mediated Scholl reaction is the key transformation to produce fully pi-conjugated („graphitized“) materials on the gram scale.⁹ Müllen and co-workers including us demonstrated that a multitude of nanographenes and GNRs can be produced this way^{4,5,10–14}, culminating in the synthesis of C₂₂₂ a PAH consisting of 37 benzene rings¹³. A main restriction is the intrinsic low solubility of extended nanographenes and GNRs due to strong aggregation by pi-pi interactions. Especially for the larger monomers solubility is a main concern but even the smallest planarized

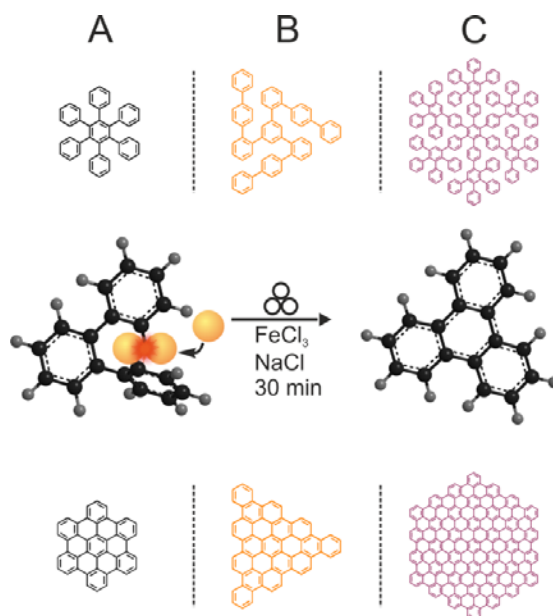


Figure 1. Scholl reaction of different polyphenylene precursors (Hexaphenylbenzene (A); C₆₀H₄₂ (B); C₂₂₂H₁₅₀ (C)) with iron(III) chloride in a planetary ball mill to produce the benchmark PAHs HBC, triangular-shaped C₆₀ and C₂₂₂. In the process 6, 9 or 54 new C-C bonds are formed. Symbol for mechanochemical reactivity is adapted from ²⁷

hexabenzocoronene (HBC) is barely soluble in common organic solvents even at elevated temperatures. GNRs face the same challenges and a common way to circumvent this, is the introduction of solubilizing groups preinstalled into the monomers.^{4,5} This presents not only additional steps in their syntheses but also a bad atom economy for the production of nanoribbons.

In the meantime, the search for the ideal, environmental friendly and preferably cheap solvents has been a persistent topic in general chemistry. But where solvent based chemistry fails other methods have to step in. In recent years mechanochemical and other solid-state methodologies have been explored as a powerful tool, offering at least as much flexibility as solvent-based processes.^{15–18} For a wide range of fields spanning everything from material synthesis^{19–23} to organic chemistry^{24–27}, fullerene chemistry^{28–30} and lately polymer chemistry^{31–35}, solvent-free pathways have been

Table 1. Reaction conditions and yields of HBC syntheses; Reaction conditions if not stated otherwise: 800 rpm, 22x 10 mm balls, ZrO₂, 12 eq. FeCl₃ per H, NaCl as bulking agent

Sample	Milling material	Milling time	Yield ^[a]
HBC-1	ZrO ₂	60 min	95 %
HBC-2	Steel	60 min	-% ^[b]
HBC-3	WC	60 min	-% ^[b]
HBC-4	Si ₃ N ₄	60 min	97 %
HBC-5	ZrO ₂	30 min	92 %
C60	ZrO ₂	60 min	81 %
C222	ZrO ₂	60 min	89 %
HBC-Ip-1	ZrO ₂	30 min	91 % ^[c]
HBC-Ip-2	ZrO ₂	30 min	45 % ^[d]

[a] yield after purification

[b] abrasion of the milling material in combination of excessive chlorination makes the determination of a yield of HBC impossible

[c] 0.3 ml of pyridine was added to capture the HCl released during the reaction

[d] 1 ml of ethanol was added to dissolve the HCl released during the reaction. Elongation of the reaction time to 60 min pushed the yield to 97%

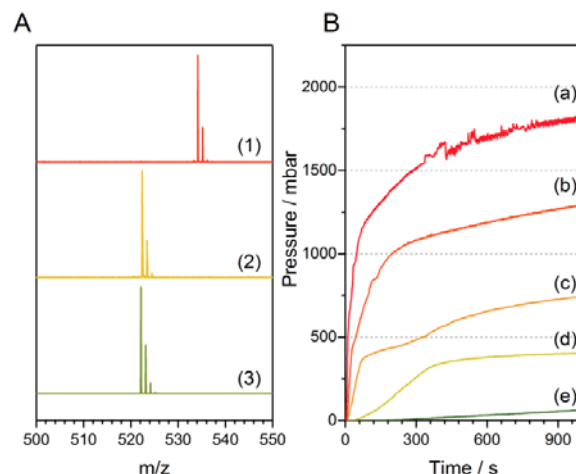


Figure 2. A: Scholl reaction of C₄₂H₃₀ to C₄₂H₁₈, milled with 22x 10 mm zirconium dioxide balls recorded MALDI-TOF spectra of HPB (1), HBC (2), and calculated MALDI-TOF spectra of HBC (3) B: Development of the vessel pressure during the milling of HPB at different milling speeds. (a) 800 rpm, (b) 600 rpm, (c) 400 rpm and (d) 200 rpm (e) 100 rpm.

developed in ball mills. While Tanner and co-workers discovered the potential of a Fe(III) catalysed oxidative coupling of 2-naphthol³⁶ it was not yet applied to more complex, insoluble systems like nanographenes. After demonstrating, that long poly(phenylene)s—which are also the precursors in PAH and GNR chemistry—can be synthesized in a ball mill the missing step towards a completely solvent-free bottom-up fabrication of GNRs lies within the cyclodehydrogenation (“graphitization”) of corresponding precursors.

In this study, we focused on developing a protocol for the solvent-free Scholl reaction under mechanochemical conditions as a versatile tool for the cyclodehydrogenation, “graphitization” of oligophenylene precursors into benchmark nanographenes such as HBC, triangular shaped C60H42 and C222 (Fig. 1). We investigated the influence of the Lewis acid/oxidation reagent, milling parameters like milling speed, ball-to-powder ratio, milling time and ball size. Furthermore, we gained a profound insight into the reaction by utilizing an advanced milling setup equipped with in-vessel temperature and pressure sensors. The quality and structural homogeneity of produced nanographenes have been confirmed by MALDI-TOF mass spectrometry and UV-Vis absorption spectroscopy.

Starting from hexaphenylbenzene (HPB), a commercially available precursor, we investigated the feasibility of the Scholl reaction under mechanochemical conditions in a planetary ball mill (PBM). It was quickly discovered, that FeCl₃ x 6 H₂O is not promoting the reaction but anhydrous FeCl₃ is. After initial experiments turned out to be very promising, we could quickly raise the yield to 95% in a 45 ml zirconium dioxide milling vessel with twenty-two 10 mm balls at 800 rpm adapting the literature known conditions for solution synthesis, of 12 eq. FeCl₃ per H atom involved in aryl-aryl bond formation (Table 1). The experiments were conducted with 0.1 g of the HPB and NaCl as bulking material (for the role of the bulking material see ESI). MALDI-TOF mass spectrometry of HBC-1 showed the most intense signal at m/z = 522 g mol⁻¹, which represents exactly the target molecule (Fig. 2A). We further conducted UV/Vis measurements (liquid and solid state) (Fig. S1) to confirm

the successful synthesis of HBC. The liquid state spectrum shows distinct peaks at 339, 357 and 385 nm which is in good agreement with the literature³⁷ while the solid state spectrum shows only one broader and slightly shifted peak at 353 nm.

After this preliminary result, we went on to study the influence of different mechanochemical parameters on the reaction. In general, the understanding of how and why they influence the mechanochemical reaction is still in its infancy.¹⁵ Several attempts have been undertaken to illuminate the processes inside the milling vessel.^{38,39} A main factor these protocols generally share is the dependence on the introduced energy.^{35,39} At first we conducted the experiment with different milling materials ranging from silicon nitride ($\rho = 3.25 \text{ g}\cdot\text{cm}^{-3}$) over zirconium dioxide ($\rho = 5.7 \text{ g}\cdot\text{cm}^{-3}$) and tempered steel ($\rho = 7.9 \text{ g}\cdot\text{cm}^{-3}$) to tungsten carbide ($\rho = 14.9 \text{ g}\cdot\text{cm}^{-3}$) to investigate the density influence of the milling material (vessel and balls) and therefore the amount of energy introduced. (Fig S2). We could observe the formation of HBC for all four milling materials (samples HBC-1 to HBC-4). However, for tempered steel and tungsten carbide, a large amount of chlorinated side product and abrasion of the milling material could be detected. Although the conditions inside the milling vessel are corrosive, we could not detect any signs of corrosion on either the milling balls or vessel made of steel. We therefore choose to continue our further investigation with the zirconium dioxide system and thereby avoiding excessive chlorination and abrasion. To rule out contamination of the product by abrasion of zirconium dioxide we conducted SEM/EDX measurements (Fig. S3). These measurements show the absence of zirconia and in addition no leftovers from the FeCl₃ used as an oxidant.

The sheer number of variables, made us turn to a design of experiment approach to determine their influence while keeping the number of experiments in a manageable range. As parameter of interest we determined the milling speed, amount of FeCl₃, milling time, ball size and filling degree (ratio of balls to powder). This investigation confirmed that indeed all of these parameters influence the reaction (Table S4 and

Fig S13) while in general a higher energy input favours a high yield of the reaction. While bigger milling balls have a negative influence on the reaction and the impact of the milling speed is rather low, raising the ball to powder ratio, milling time and equivalents of iron (III) chloride all lead to an increased yield (Fig. S13 top). Increasing the eq. of iron (III) chloride leads to a reduced reaction time until full conversion. The optimised condition for the mechanochemical Scholl-reaction of HPB are: 10 mm milling balls, 800 rpm, a ball to powder ratio of 45, 72 eq. of iron FeCl_3 and 30 minutes of milling (sample HBC-5, run 18 in the DOE). In an additional trial we demonstrated, that an increase of milling time consequently leads to a higher percentage of chlorinated side products (Fig S4). It is therefore of key interest to track the reaction and determine its end in order to obtain the cleanest product possible.

Since steep limitations on in-situ analysis methods are imposed by the synthesis protocol, the ball mill is commonly referred to as a "black box" and in-situ data is generally scarce and hard to obtain.⁴⁰⁻⁴⁵ Lately, we have shown that in-situ temperature measurements can give indications on the progress of a reaction.^{33,34,46} While the merit of this method is currently being discussed⁴⁷, in the case of the Scholl reaction the temperature rise resulting from the reaction enthalpy, however, is marginal because of the small amount of reactant and cannot be used to track the progress in a satisfying manner (Fig. S5). Therefore, we reverted to the in-situ pressure measurement of the milling vessel, which are much less controversial, to elucidate the reaction further. Applied to our system, we can observe a step rise of pressure in the first minutes of the reaction (Fig. 2B). Caused by the release of HCl during the reaction, this rise occurs in different slopes depending on the milling speed (Fig. S6). As expected the reaction proceeds the slowest at low energy input, but even at 200 rpm a plateau is reached after as little as 10 minutes. While for 100 rpm no reaction can be observed at all. The higher absolute pressure for higher milling speeds are caused by the increasing temperatures of the vessels, an effect more profound for higher milling speeds (Fig. S5). In order to verify these results, we conducted experiments without HPB in the mixture (Fig. S7) and observed only a neglectable overpressure due to the heating of the vessel.

In order to establish our method as a versatile alternative to the classical process it is important to broaden the scope to bigger nanographenes. The syntheses towards C_{60} and C_{222} were subsequently investigated in solvent-free conditions. For both systems similar results could be achieved with the slightly altered parameters compared to HPB (Fig. 3, Table 1). In the solid state UV/VIS spectra (Fig. S1 A) the maxima show a clear bathochromic shift to 395 nm for C_{60} and to 717 nm for C_{222} . In both cases the yield of the optimized classical solvent based procedures are rather low (C_{60} – 71%⁴⁸ and C_{222} – 62%¹³) whereas the solvent-free approach optimized for HPB already leads to yields of 81% and 89%, respectively. The in-situ investigations of these systems reveal that even for the bigger molecules the reaction proceeds in a matter of minutes (SFig 8). This is especially surprising, since C_{222} is - up to now - the biggest reported PAH with well-defined structure and its planarization took 24 hours under optimised conditions,¹³ whereas our protocol for HPB can be transferred without extensive adaption and therefore seems to be independent of precursor size.

Furthermore, we obtained promising results (a yield of 58% of HBC after 30 minutes) with a proof-of-principle experiment in a mixer ball mill (MM) - a mill type more common in organic laboratories (more details in the ESI). Independent of the milling technique another challenge we faced was the build-up of pressure during the reaction. In order to reduce the pressure we followed two strategies, namely the capture of the HCl with pyridine (HBC-lp-1) and the dissolution of the HCl in a small amount of ethanol introduced into the vessel (HBC-lp-2). While both succeeded in reducing the pressure in the system (SFig. 9) the addition of solvent seemed to slow down the reaction and therefore led to a low yield of 45% (Table 1). An elongation of the reaction time to one hour already pushed the yield to 97% while eliminating the overpressure. For HBC-lp-1 however the yield after 30 minutes (91%) is similar to HBC-5 milled under the same conditions.

In summary, we described a novel and innovative mechanochemical process for the Scholl reaction of benchmark nanographenes. Using FeCl_3 in a solvent-free protocol in a planetary ball mill, we could demonstrate that these reactions proceed in as little as 30 minutes and are limited by neither the solubility nor the size of the PAH. Utilizing MALD-TOF and solid state UV/Vis measurements to prove the success of the reaction also lead to the discovery of growing degree of chlorination with increasing reaction time. Based on these findings, we explored the influence of different milling parameters on our reaction and found that energy related parameters play a key role. Utilizing in-situ pressure measurements we further elucidated the reaction and determined a threshold milling speed for the process. Furthermore, we expanded our protocol to bigger nanographenes, namely C_{60} and C_{222} . In addition, we also transferred the process to a mixer ball mill enabling the scalability to few mg scales. This new reaction route paves the way towards larger extended nanographenes in spite of their

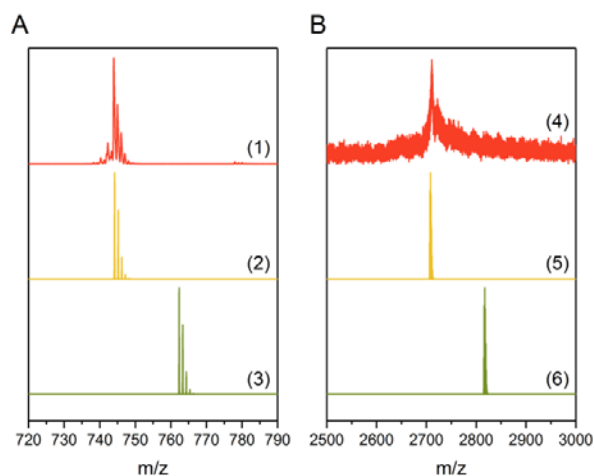


Figure 3. A: Scholl reaction of $\text{C}_{60}\text{H}_{42}$ to $\text{C}_{60}\text{H}_{24}$, recorded MALDI-TOF spectrum of $\text{C}_{60}\text{H}_{24}$ (1), calculated MALDI-TOF spectra of $\text{C}_{60}\text{H}_{24}$ (2) and $\text{C}_{60}\text{H}_{42}$ (3). B: Scholl reaction of $\text{C}_{222}\text{H}_{150}$ to $\text{C}_{222}\text{H}_{42}$, recorded MALDI-TOF spectra of $\text{C}_{222}\text{H}_{42}$ (4), calculated MALDI-TOF spectra of $\text{C}_{222}\text{H}_{42}$ (5) and $\text{C}_{222}\text{H}_{150}$ (6).

low solubility and therefore renders the introduction of solubilizing groups obsolete.

We gratefully acknowledge financial support from the Federal Ministry of Education and Research (BMBF) for support of the Mechanocarb project (award number 03SF0498), ERC grants on 2DMATER, the EC under Graphene Flagship (No. CNECT-ICT604391), the Center for Advancing Electronics Dresden (cfaed), the European Social Fund, and the Federal State of Saxony (ESF-Project "GRAPHD", TU Dresden). The authors acknowledge Sebastian Ehrling for the SEM/EDX measurements and Dr. Ajayakumar Murugan Rathamony for synthetic support.

Conflicts of interest

There are no conflicts to declare.

Notes and references

- 1 B. T. King, J. Kroulík, C. R. Robertson, P. Rempala, et al., *J. Org. Chem.*, 2007, **72**, 2279–2288.
- 2 M. Grzybowski, K. Skonieczny, H. Butenschön and D. T. Gryko, *Angew. Chemie Int. Ed.*, 2013, **52**, 9900–9930.
- 3 R. Scholl, C. Seer and R. Weitzenböck, *Berichte der Dtsch. Chem. Gesellschaft*, 1910, **43**, 2202–2209.
- 4 A. Narita, X.-Y. Wang, X. Feng and K. Müllen, *Chem. Soc. Rev.*, 2015, **44**, 6616–6643.
- 5 A. Narita, X. Feng and K. Müllen, *Chem. Rec.*, 2015, **15**, 295–309.
- 6 L. Talirz, P. Ruffieux and R. Fasel, *Adv. Mater.*, 2016, **28**, 6222–6231.
- 7 J. Cai, P. Ruffieux, R. Jaafar, M. Bieri, et al., *Nature*, 2010, **466**, 470–473.
- 8 M. Treier, C. A. Pignedoli, T. Laino, R. Rieger, et al., *Nat. Chem.*, 2011, **3**, 61–67.
- 9 T. H. Vo, M. Shekhirev, D. A. Kunkel, M. D. Morton, et al., *Nat. Commun.*, 2014, **5**, 3189.
- 10 L. Chen, Y. Hernandez, X. Feng and K. Müllen, *Angew. Chemie Int. Ed.*, 2012, **51**, 7640–7654.
- 11 A. Narita, X. Feng, Y. Hernandez, S. A. Jensen, et al., *Nat. Chem.*, 2013, **6**, 126–132.
- 12 M. D. Watson, A. Fechtenkötter and K. Müllen, *Chem. Rev.*, 2001, **101**, 1267–1300.
- 13 C. D. Simpson, J. D. Brand, A. J. Berresheim, L. Przybilla, et al., *Chem. - A Eur. J.*, 2002, **8**, 1424–1429.
- 14 C. D. Simpson, G. Matternsteig, K. Martin, L. Gherghel, et al., *J. Am. Chem. Soc.*, 2004, **126**, 3139–3147.
- 15 J.-L. Do and T. Friščić, *Synlett*, 2017, **28**, 2066–2092.
- 16 S. L. James and T. Friščić, *Chem. Soc. Rev.*, 2013, **42**, 7494–7496.
- 17 J. G. Hernández and C. Bolm, *J. Org. Chem.*, 2017, **82**, 4007–4019.
- 18 S. L. James, C. J. Adams, C. Bolm, D. Braga, et al., *Chem. Soc. Rev.*, 2012, **41**, 413–447.
- 19 K. Užarević, T. C. Wang, S.-Y. Moon, A. M. Fidelli, et al., *Chem. Commun.*, 2016, **52**, 2133–2136.
- 20 W. Yuan, T. Friščić, D. Apperley and S. L. James, *Angew. Chemie*, 2010, **122**, 4008–4011.
- 21 W. Shi, J. Yu, Z. Jiang, Q. Shao, et al., *Beilstein J. Org. Chem.*, 2017, **13**, 1661–1668.
- 22 C. Schneidermann, N. Jäckel, S. Oswald, L. Giebeler, et al., *ChemSusChem*, 2017, **10**, 2416–2424.
- 23 D. Leistenschneider, N. Jäckel, F. Hippauf, V. Presser, et al., *Beilstein J. Org. Chem.*, 2017, **13**, 1332–1341.
- 24 F. Bernhardt, R. Trotzki, T. Szuppa, A. Stolle, et al., *Beilstein J. Org. Chem.*, 2010, **6**, No. 7.
- 25 A. Stolle, T. Szuppa, S. E. S. Leonhardt and B. Ondruschka, *Chem. Soc. Rev.*, 2011, **40**, 2317–2329.
- 26 G. N. Hermann, P. Becker and C. Bolm, *Angew. Chemie*, 2015, **127**, 7522–7525.
- 27 N. R. Rightmire and T. P. Hanusa, *Dalt. Trans.*, 2016, **45**, 2352–2362.
- 28 K. Komatsu, K. Fujiwara and Y. Murata, *Chem. Commun.*, 2000, **17**, 1583–1584.
- 29 K. Komatsu, G.-W. Wang, Y. Murata, T. Tanaka, et al., *J. Org. Chem.*, 1998, **63**, 9358–9366.
- 30 G.-W. Wang, K. Komatsu, Y. Murata and M. Shiro, *Nature*, 1997, **387**, 583–586.
- 31 P. Zhang and S. Dai, *J. Mater. Chem. A*, 2017, **5**, 16118–16127.
- 32 N. Ohn, J. Shin, S. S. Kim and J. G. Kim, *ChemSusChem*, 2017, **10**, 3529–3533.
- 33 S. Grätz, B. Wolfrum and L. Borchardt, *Green Chem.*, 2017, **19**, 2973–2979.
- 34 E. Troschke, S. Grätz, T. Lübken and L. Borchardt, *Angew. Chemie*, 2017, **129**, 6963–6967.
- 35 S. Grätz and L. Borchardt, *RSC Adv.*, 2016, **6**, 64799–64802.
- 36 M. O. Rasmussen, O. Axelsson and D. Tanner, *Synth. Commun.*, 1997, **27**, 4027–4030.
- 37 W. Hendel, Z. H. Khan and W. Schmidt, *Tetrahedron*, 1986, **42**, 1127–1134.
- 38 T. Szuppa, A. Stolle, B. Ondruschka and W. Hopfe, *ChemSusChem*, 2010, **3**, 1181–1191.
- 39 T. Szuppa, A. Stolle, B. Ondruschka and W. Hopfe, *Green Chem.*, 2010, **12**, 1288–1294.
- 40 S. Haferkamp, F. Fischer, W. Kraus and F. Emmerling, *Beilstein J. Org. Chem.*, 2017, **13**, 2010–2014.
- 41 L. Batzdorf, F. Fischer, M. Wilke, K.-J. Wenzel, et al., *Angew. Chemie Int. Ed.*, 2015, **54**, 1799–1802.
- 42 P. A. Julien, I. Malvestiti and T. Friščić, *Beilstein J. Org. Chem.*, 2017, **13**, 2160–2168.
- 43 K. S. McKissic, J. T. Caruso, R. G. Blair and J. Mack, *Green Chem.*, 2014, **16**, 1628–1632.
- 44 F. Schneider, T. Szuppa, A. Stolle, B. Ondruschka, et al., *Green Chem.*, 2009, **11**, 1894–1899.
- 45 R. Schmidt, H. Martin Scholze and A. Stolle, *Int. J. Ind. Chem.*, 2016, **7**, 181–186.
- 46 H. Kulla, M. Wilke, F. Fischer, M. Röllig, et al., *Chem. Commun.*, 2017, **53**, 1664–1667.
- 47 K. Užarević, N. Ferdelji, T. Mrla, P. A. Julien, et al., *Chem. Sci.*, 2018, **9**, 2525–2532.
- 48 X. Feng, J. Wu, M. Ai, W. Pisula, et al., *Angew. Chemie*, 2007, **119**, 3093–3096.